

# Evaluation of a Passive Heat Exchanger Based Cooling System for Fuel Cell Applications

*Anthony J. Colozza*  
*Analex Corporation, Cleveland, Ohio*

*Kenneth A. Burke*  
*Glenn Research Center, Cleveland, Ohio*

## NASA STI Program . . . in Profile

Since its founding, NASA has been dedicated to the advancement of aeronautics and space science. The NASA Scientific and Technical Information (STI) program plays a key part in helping NASA maintain this important role.

The NASA STI Program operates under the auspices of the Agency Chief Information Officer. It collects, organizes, provides for archiving, and disseminates NASA's STI. The NASA STI program provides access to the NASA Aeronautics and Space Database and its public interface, the NASA Technical Reports Server, thus providing one of the largest collections of aeronautical and space science STI in the world. Results are published in both non-NASA channels and by NASA in the NASA STI Report Series, which includes the following report types:

- **TECHNICAL PUBLICATION.** Reports of completed research or a major significant phase of research that present the results of NASA programs and include extensive data or theoretical analysis. Includes compilations of significant scientific and technical data and information deemed to be of continuing reference value. NASA counterpart of peer-reviewed formal professional papers but has less stringent limitations on manuscript length and extent of graphic presentations.
- **TECHNICAL MEMORANDUM.** Scientific and technical findings that are preliminary or of specialized interest, e.g., quick release reports, working papers, and bibliographies that contain minimal annotation. Does not contain extensive analysis.
- **CONTRACTOR REPORT.** Scientific and technical findings by NASA-sponsored contractors and grantees.

- **CONFERENCE PUBLICATION.** Collected papers from scientific and technical conferences, symposia, seminars, or other meetings sponsored or cosponsored by NASA.
- **SPECIAL PUBLICATION.** Scientific, technical, or historical information from NASA programs, projects, and missions, often concerned with subjects having substantial public interest.
- **TECHNICAL TRANSLATION.** English-language translations of foreign scientific and technical material pertinent to NASA's mission.

Specialized services also include creating custom thesauri, building customized databases, organizing and publishing research results.

For more information about the NASA STI program, see the following:

- Access the NASA STI program home page at <http://www.sti.nasa.gov>
- E-mail your question via the Internet to [help@sti.nasa.gov](mailto:help@sti.nasa.gov)
- Fax your question to the NASA STI Help Desk at 443-757-5803
- Telephone the NASA STI Help Desk at 443-757-5802
- Write to:  
NASA Center for AeroSpace Information (CASI)  
7115 Standard Drive  
Hanover, MD 21076-1320



# Evaluation of a Passive Heat Exchanger Based Cooling System for Fuel Cell Applications

*Anthony J. Colozza*  
*Analex Corporation, Cleveland, Ohio*

*Kenneth A. Burke*  
*Glenn Research Center, Cleveland, Ohio*

National Aeronautics and  
Space Administration

Glenn Research Center  
Cleveland, Ohio 44135

Trade names and trademarks are used in this report for identification only. Their usage does not constitute an official endorsement, either expressed or implied, by the National Aeronautics and Space Administration.

*Level of Review:* This material has been technically reviewed by technical management.

Available from

NASA Center for Aerospace Information  
7115 Standard Drive  
Hanover, MD 21076-1320

National Technical Information Service  
5301 Shawnee Road  
Alexandria, VA 22312

Available electronically at <http://gltrs.grc.nasa.gov>

# **Evaluation of a Passive Heat Exchanger Based Cooling System for Fuel Cell Applications**

Anthony J. Colozza  
Analex Corporation  
Cleveland, Ohio 44135

Kenneth A. Burke  
National Aeronautics and Space Administration  
Glenn Research Center  
Cleveland, Ohio 44135

## **Abstract**

Fuel cell cooling is conventionally performed with an actively controlled, dedicated coolant loop that exchanges heat with a separate external cooling loop. To simplify this system the concept of directly cooling a fuel cell utilizing a coolant loop with a regenerative heat exchanger to preheat the coolant entering the fuel cell with the coolant exiting the fuel cell was analyzed. The preheating is necessary to minimize the temperature difference across the fuel cell stack. This type of coolant system would minimize the controls needed on the coolant loop and provide a mostly passive means of cooling the fuel cell. The results indicate that an operating temperature of near or greater than 70 °C is achievable with a heat exchanger effectiveness of around 90 percent. Of the heat exchanger types evaluated with the same type of fluid on the hot and cold side, a counter flow type heat exchanger would be required which has the possibility of achieving the required effectiveness. The number of heat transfer units required by the heat exchanger would be around 9 or greater. Although the analysis indicates the concept is feasible, the heat exchanger design would need to be developed and optimized for a specific fuel cell operation in order to achieve the high effectiveness value required.

## **Introduction**

In previous work (Ref. 1), it has been shown that high thermal conductivity cooling plates can be utilized to remove heat generated within a fuel cell. One of the advantages of utilizing this type of cooling approach is that a generic cooling loop can be utilized. The fuel cell cooling system does not impose any conditions on this generic cooling loop, such as temperature or flow rate. The cooling flow from the generic loop is adjusted through the use of a valve so that the internal temperature of the fuel cell is maintained at the desired level. A conductive plate system as compared to the more conventional fluid cooling system for a fuel cell is shown in Figure 1. The cooling plate system utilizes a manifold to exchange heat between the cooling plates and the cooling fluid. Because of the high thermal conductivity cooling plates, they effectively spread the heat being transferred to the cooling manifold (heat exchanger) and will maintain a uniform temperature gradient across their surface. This temperature uniformity is maintained even though the inlet coolant flow temperature to the manifold is much lower than the manifold exit coolant flow temperature.

Another alternative method to the conventional cooling loop system utilizes the internal fuel cell coolant flow channels, as the conventional system does, but operates with a generic cooling loop similar to that used with the conductive cooling plate system. The main issue with utilizing an external cooling loop to directly cool the fuel cell is the temperature of the cooling fluid into the stack. As with the cooling plate system, the coolant flow into the fuel cell can be controlled with a valve regulating it to maintain the proper flow rate to maintain an exit temperature set point. However, considering that the coolant loop fluid temperature will be around 25 °C and the desired operating temperature of the fuel cell will be

approximately 70 °C, the low inlet temperature from the cooling loop will cause a significant temperature gradient within the fuel cell from the area where the coolant enters the fuel cell to where it exits.

The conventional internal cooling system can be simplified to a mostly passive, single fluid system through the use of a heat exchanger between the incoming and exiting fluid flow. This heat exchanger would increase the temperature or preheat the inlet coolant flow into the fuel cell to maintain a low temperature difference across the fuel cell stack. A flow control valve, similar to that of the cooling plate system, would control the heat removal from the fuel cell. This concept is shown in Figure 2.

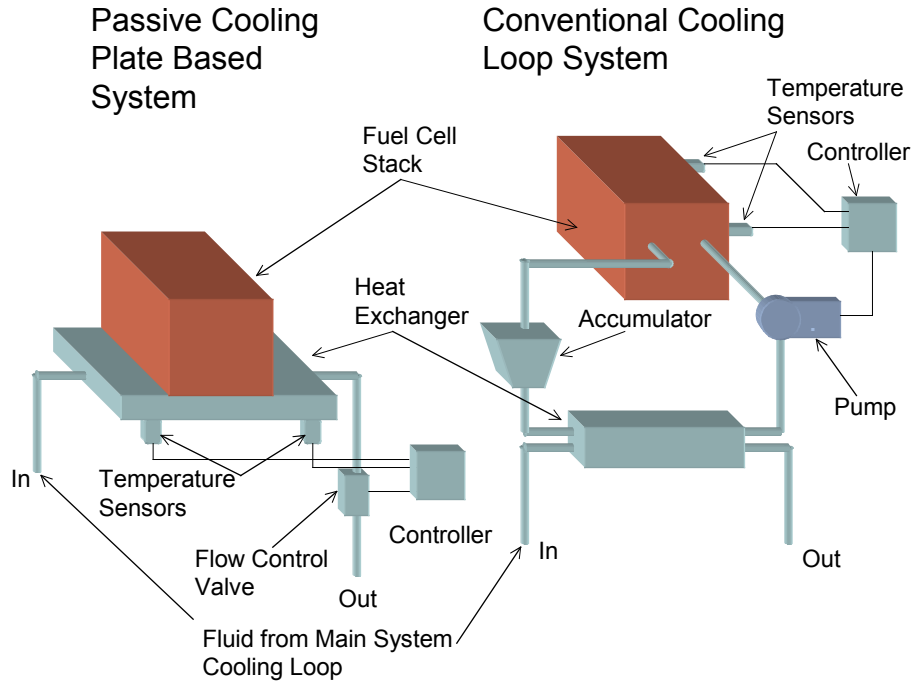


Figure 1.—Comparison between a conventional fuel cell cooling system and the cooling plate based system (Ref. 1).

### Passive Heat Exchanger Based Cooling System

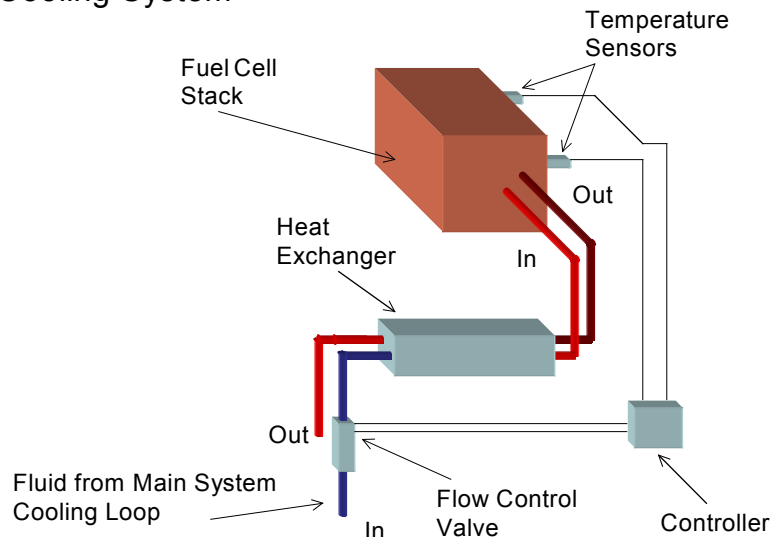


Figure 2.—Heat exchanger cooling system concept diagram.

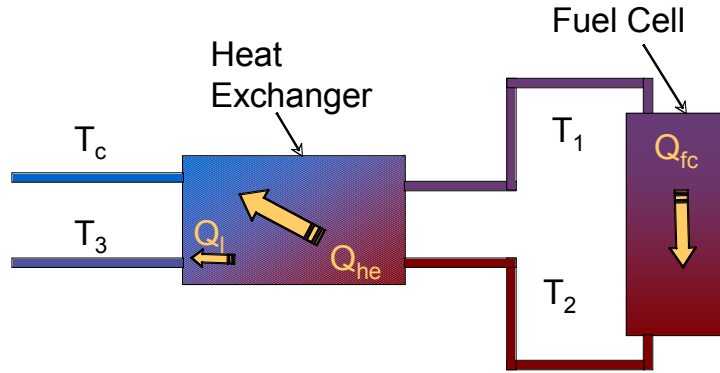


Figure 3.—Heat exchanger cooling system temperature and flow layout.

### Analysis

The effectiveness of the heat exchanger is the key aspect to the feasibility of this concept. Enough heat must be transferred from the warm exit coolant to the cool inlet coolant to bring the temperature difference between the inlet and outlet coolant flow within the desired fuel cell operating range while maintaining sufficient coolant flow rate through the fuel cell and heat exchanger to remove the excess heat generated by the fuel cell during operation.

To evaluate this concept and assess its feasibility, an energy balance approach was utilized. The waste heat of the fuel cell adds energy to the coolant flow thus raising the temperature of the coolant flow. This flow then passes through the heat exchanger and transfers some of its heat to the incoming coolant flow, thereby increasing the fuel cell inlet coolant temperature. The heat transferred by the heat exchanger will depend on the effectiveness of the heat exchanger ( $\epsilon$ ). The heat exchanger effectiveness is a comparison between the actual rate of heat transfer between the hot and cold fluids to the maximum possible heat transfer rate for an infinitely sized heat exchanger. The flow rate through the fuel cell, and subsequently through the heat exchanger, is determined by the desired temperature difference across the fuel cell ( $\Delta T_{fc}$ ) and the heat being generated by the fuel cell ( $Q_{fc}$ ).

Initially, when the fuel cell is turned on and the coolant flow is started, the fuel cell coolant inlet temperature ( $T_1$ ) is near that of the heat exchanger inlet coolant temperature ( $T_c$ ). As the fuel cell operates, the fuel cell imparts waste heat into the exit coolant flow before the heat exchanger transfers it to the inlet coolant flow. This raises the inlet temperature of the coolant to the fuel cell. Eventually a steady state condition develops between the heat exchanger inlet coolant temperature, the fuel cell inlet coolant temperature, and nominal fuel cell stack temperature. This process is illustrated in Figure 3.

The resultant steady state temperature of the fuel cell inlet coolant will depend on the effectiveness of the heat exchanger in transferring heat from the fuel cell coolant outlet back to the fuel cell inlet coolant flow. To get to the steady state coolant temperature, the analysis is run through a number of steps “ $i$ ” until a steady state is reached. The heat transfer through the heat exchanger, in each step of the process, is given by Equation (1) (Ref. 2)

$$Q_{he_i} = \epsilon \dot{m} c_p (T_{2_{i-1}} - T_c) \quad (1)$$

The coolant mass flow ( $\dot{m}$ ), given by Equation (2), is set by the desired fuel cell temperature difference, heat being produced by the fuel cell and the specific heat of the coolant at STP ( $c_p$ ).

$$\dot{m} = \frac{Q_{fc}}{c_p \Delta T_{fc}} \quad (2)$$

From Equations (1) and (2) the temperature of the coolant into and out of the fuel cell ( $T_{1i}$  and  $T_{2i}$  respectively), can be determined for each incremental step in the analysis. These temperatures are given by Equations (3) and (4) respectively.

$$T_{1i} = \frac{Q_{he_i}}{\dot{m}c_p} + T_c \quad (3)$$

$$T_{2i} = \frac{Q_{fc}}{\dot{m}c_p} + T_{1i} \quad (4)$$

The effectiveness of the heat exchanger limits the amount of heat transferred back to the coolant loop. Therefore some heat is lost. This heat loss ( $Q_{li}$ ) and the subsequent exit temperature ( $T_{3i}$ ) of the coolant from the heat exchanger are calculated by Equations (5) and (6) respectively.

$$Q_{li} = \frac{Q_{he_i}}{\varepsilon} (1 - \varepsilon) \quad (5)$$

$$T_{3i} = T_c + \frac{Q_{li}}{\dot{m}c_p} \quad (6)$$

The above equations can be combined to provide an expression for the inlet coolant temperature of the fuel cell for each time step ‘ $i$ ’. This provides an expression for the inlet temperature as a function of the heat exchanger effectiveness, inlet cooling temperature and temperature difference across the fuel cell given in Equation (7) with the initial condition, at  $i=0$ , given in Equation (8). The variables used in this equation specify the operating conditions for the fuel cell and heat exchanger.

$$T_{1i} = \varepsilon(\Delta T_{fc} + T_{1_{i-1}}) + T_c(1 - \varepsilon) \quad (7)$$

$$T_{1_{i=0}} = T_c \quad (8)$$

Equation (7) was solved for heat exchanger effectiveness values that ranged from 40 to 90 percent and for various coolant temperatures and difference between the fuel cell inlet and outlet coolant temperature. These results are shown in Figures 4 through 6. In these figures, inlet temperature is plotted as a function of the time step, which in this case is in seconds. After a number of time steps a steady state condition will be reached.

In the following figures, it can be seen that the rate at which the steady state inlet temperature is reached is dependent on the effectiveness of the heat exchanger. The higher the effectiveness, the longer it takes to reach a steady state condition. Four cases were shown where variations in the coolant temperature and temperature difference were examined. Increasing the coolant loop temperature and/or the temperature difference across the fuel cell stack increased the fuel cell coolant inlet temperature. This in turn increases the operating temperature of the fuel cell.

The steady state inlet temperature defines the operating temperature of the fuel cell once this steady state is achieved, for a given heat exchanger effectiveness. Figure 8 shows the effect of coolant temperature and fuel cell temperature difference on the steady state temperature for each of the cases given in Figures 4 through 7.

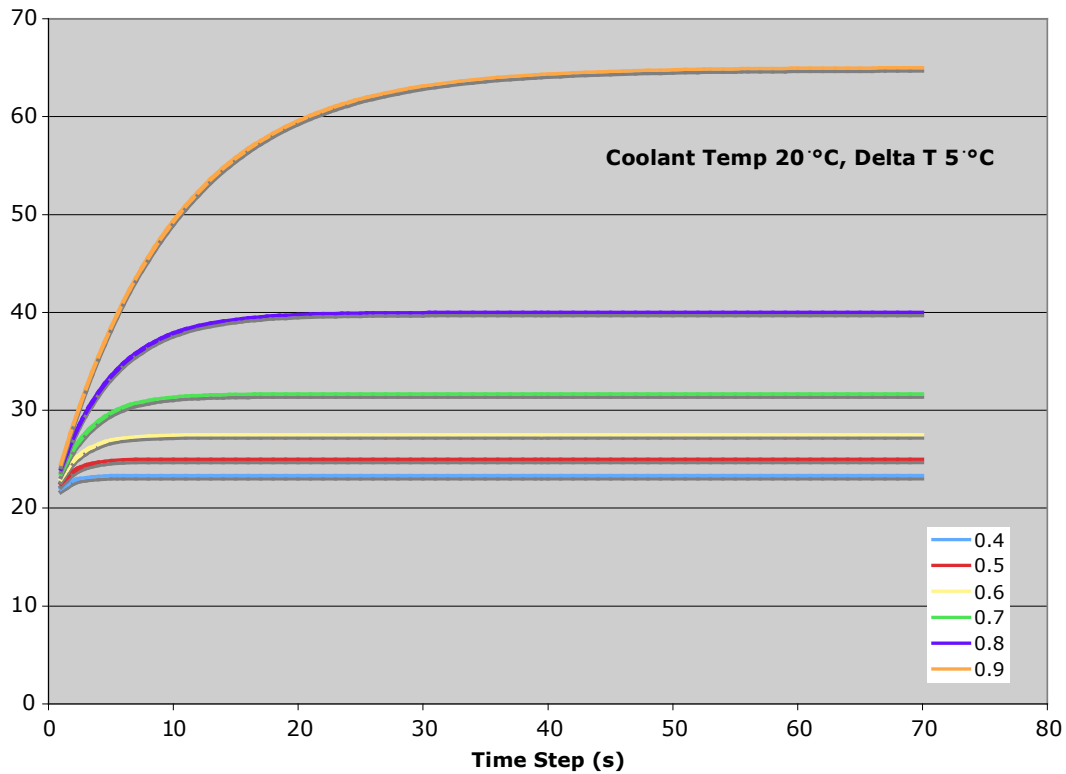


Figure 4.—Fuel cell inlet temperature with a coolant temperature of 20 °C and 5 °C temperature difference across the fuel cell for heat exchanger effectiveness values of 0.4 through 0.9.

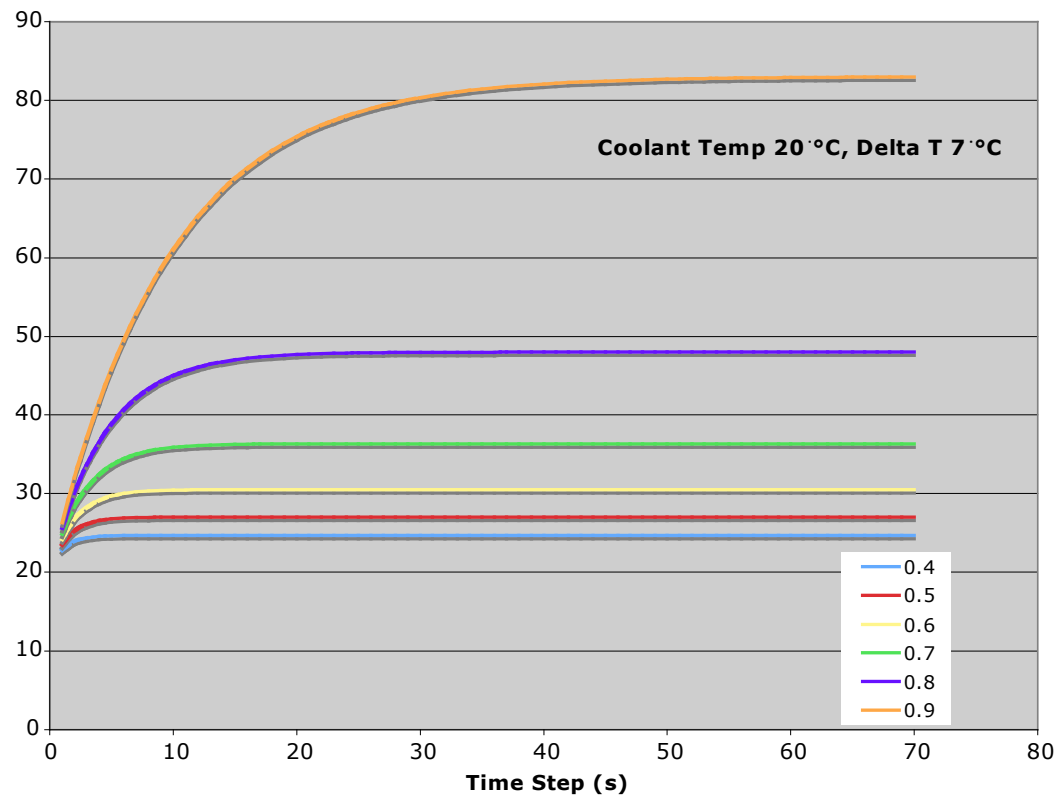


Figure 5.—Fuel cell inlet temperature with a coolant temperature of 20 °C and 7 °C temperature difference across the fuel cell for heat exchanger effectiveness values of 0.4 through 0.9.

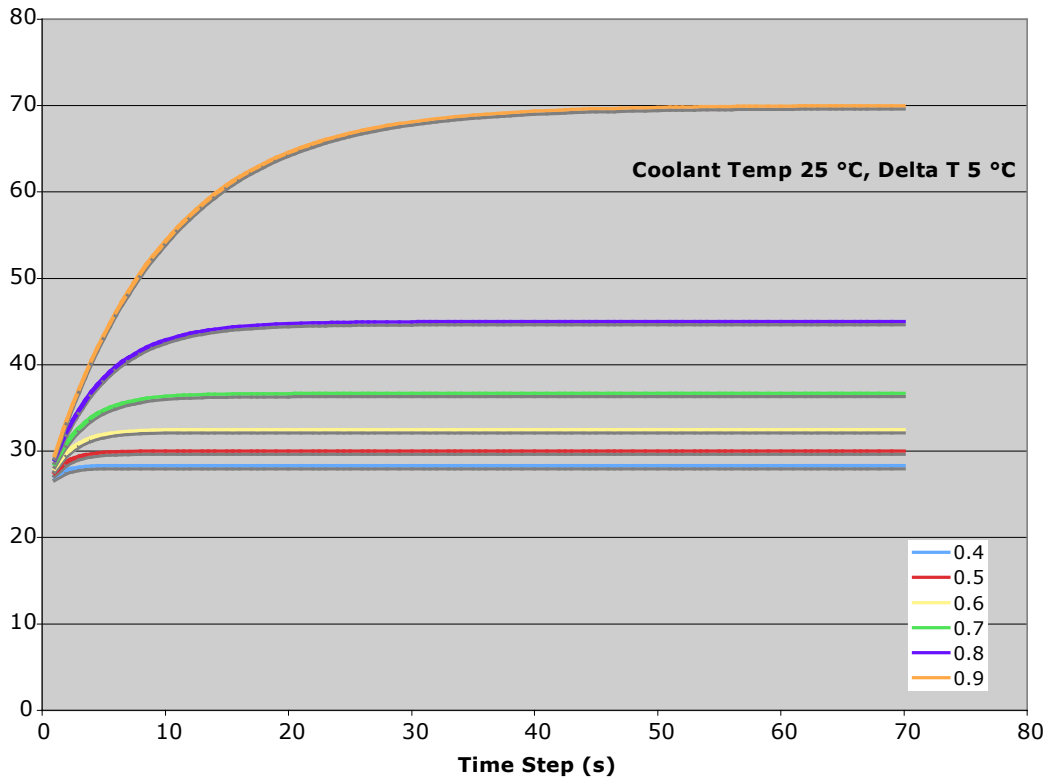


Figure 6.—Fuel cell inlet temperature with a coolant temperature of 20 °C and 7 °C temperature difference across the fuel cell for heat exchanger effectiveness values of 0.4 through 0.9.

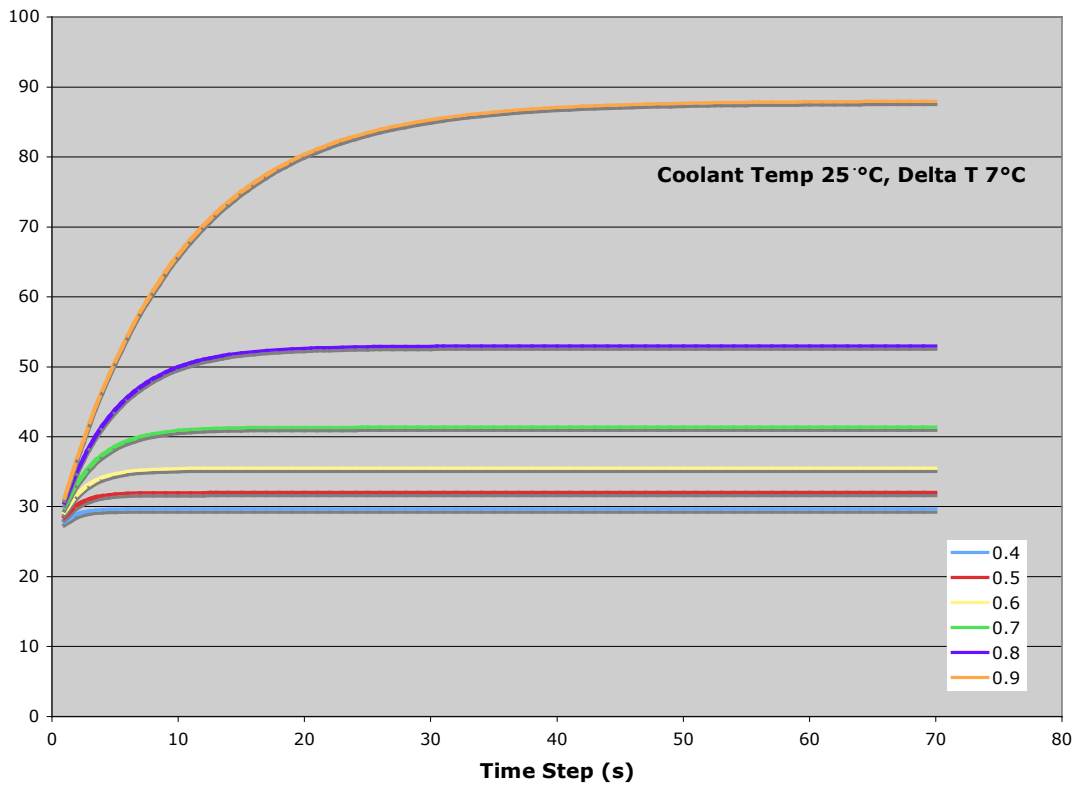


Figure 7.—Fuel cell inlet temperature with a coolant temperature of 20 °C and 7 °C temperature difference across the fuel cell for heat exchanger effectiveness values of 0.4 through 0.9.

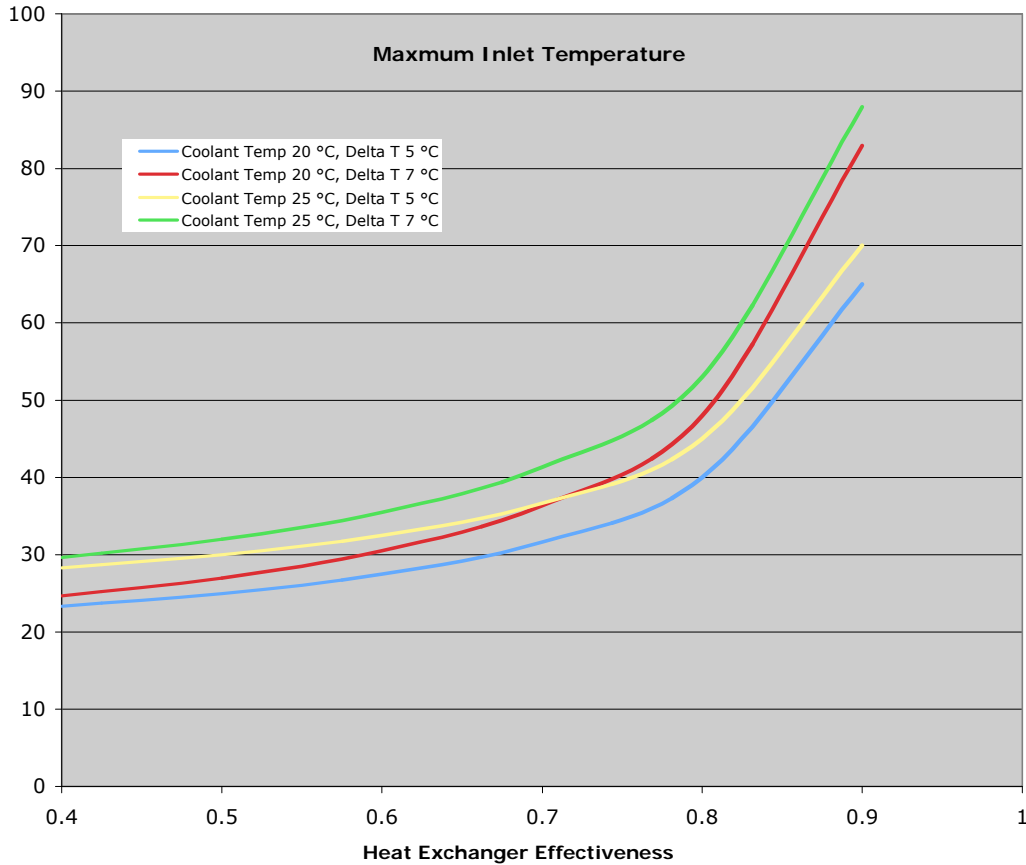


Figure 8.—Steady state maximum fuel cell inlet coolant temperature.

From Figure 8, it can be seen that increasing the coolant temperature and/or the temperature difference across the fuel cell can provide a considerable increase in the inlet temperature of the coolant and therefore minimum operating temperature of the fuel cell.

For a minimum operating temperature of 65 °C, the required heat exchanger effectiveness will decrease from approximately 0.91 to 0.84 by increasing the coolant loop temperature from 20 to 25 °C and increasing the temperature difference across the fuel cell from 5 to 7 °C.

## Heat Exchanger Design

For this concept to be viable, the heat exchanger design must meet the effectiveness requirements determined in the previous section. At a minimum, the heat exchanger effectiveness will need to be 0.84 or higher. This number is dependent on the desired temperature difference within the fuel cell, desired operating temperature, and available heat exchanger inlet coolant temperature. A smaller temperature difference, lower heat exchanger inlet coolant temperature, or higher fuel cell operating temperature will each increase the required heat exchanger effectiveness.

The heat exchanger design is constrained by the proposed design concept. The cold fluid entering the heat exchanger is the same as the hot fluid. Therefore their specific heat values or fluid capacity rates ( $C_h$  {W/K} for the hot fluid and  $C_c$  {W/K} for the cold fluid) are the same as given in Equation (9).

$$\frac{C_h}{C_c} = 1 \quad (9)$$

For a fluid capacity rate ratio of 1, the theoretical effectiveness for various types of heat exchangers are known as a function of the number of heat transfer units ( $N_{tu}$ ), given by Equation (10) (Ref. 3). This equation is based on the heat exchanger fluid heat transfer surface area ( $A$  {m<sup>2</sup>}), the thermal conductance from one fluid to the next ( $U$ , {W/m<sup>2</sup>K}), and the fluid capacity rate ( $C$ , {W/K}).

$$N_{tu} = \frac{AU}{C} \quad (10)$$

The number of heat transfer units is a non-dimensional quantity that expresses the heat transfer capability or size of the heat exchanger (Ref. 3). In general the smaller the number of heat transfer units, the lower the effectiveness of the heat exchanger. As the value of  $N_{tu}$  increases, the heat transfer effectiveness will asymptotically approach a limit based on the heat exchanger configuration. Theoretical data on the heat exchanger effectiveness for various types of heat exchangers, given in Reference 1, was used to assess their applicability to the heat exchanger requirements for this concept. A number of types of heat exchangers were considered. The simplest designs were a counter flow and parallel flow heat exchanger. In these designs the hot and cold fluids flow in separate tubes or channels. In the counter flow design they flow in opposite directions where as in the parallel design they flow in the same direction, as shown in Figures 9 and 10 respectively.

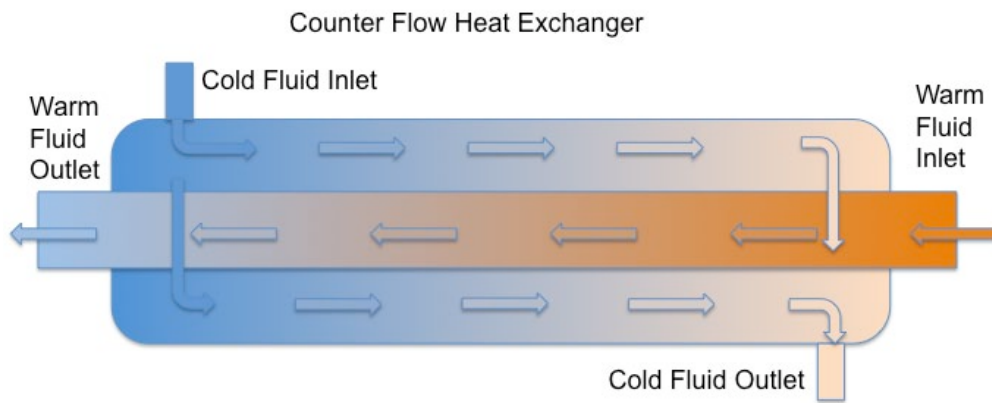


Figure 9.—Illustration of a counter flow heat exchanger.

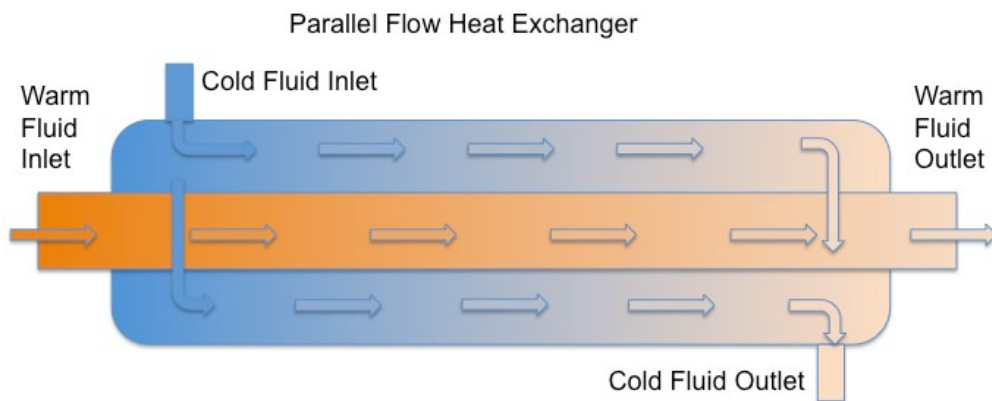


Figure 10.—Illustration of a parallel flow heat exchanger.

A similar design to the counter flow and parallel flow heat exchangers is a cross flow heat exchanger. In a cross flow design, the warm fluid enters the heat exchanger 90° from the cold fluid. There are three variations of this design approach. The first is where both the hot and cold fluids are unmixed as they travel through the heat exchanger in discrete individual passages. All the heat transfer takes place through the passage walls. The second type of cross flow heat exchanger is where one of the fluids is allowed to mix within a dedicated chamber adjacent to the passages for the second fluid and is not constrained to individual passages. And the third variation is where both fluids are in adjacent separate chambers but each fluid is allowed to mix and is not constrained to individual passageways. The cross flow heat exchanger is illustrated in Figure 11.

The next type of configuration combines both the parallel and counter flow heat exchangers. Fluid enters and exits from the same side of the heat exchanger and follows a U-shaped path within the heat exchanger. Part of the flow is counter flow to the cold fluid and part is parallel. The cold fluid is mixed and flows over the inner hot fluid tubes contained by an outer shell. This design is illustrated in Figure 12. The illustration shows one counter and parallel pass however this type of heat exchanger can be constructed with multiple passes through a serpentine path before exiting.

The last heat exchanger configuration, shown in Figure 13, is a split flow type. This configuration is similar to the parallel-counter flow design, show in Figure 12, except that the entrance for the cold fluid is at the center of the heat exchanger and there are two exits. Portions operate similarly to both parallel and counter flow heat exchangers. As with the parallel-counter flow design, the cooling fluid flows in an outer shell and is mixed while the warm fluid passes through a U-shaped tube.

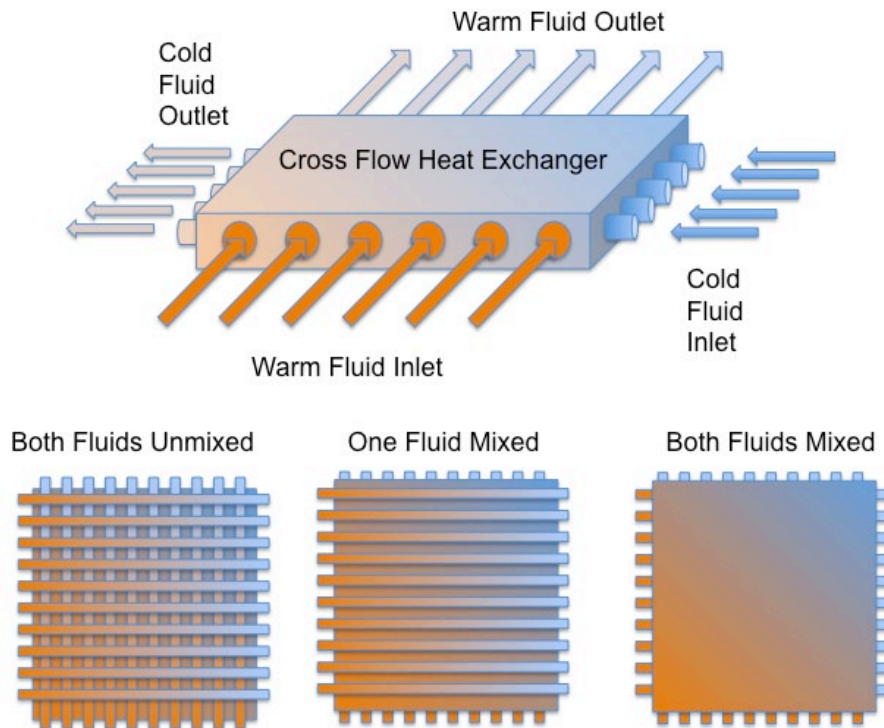


Figure 11.—Illustration of a cross flow heat exchanger and its variations.

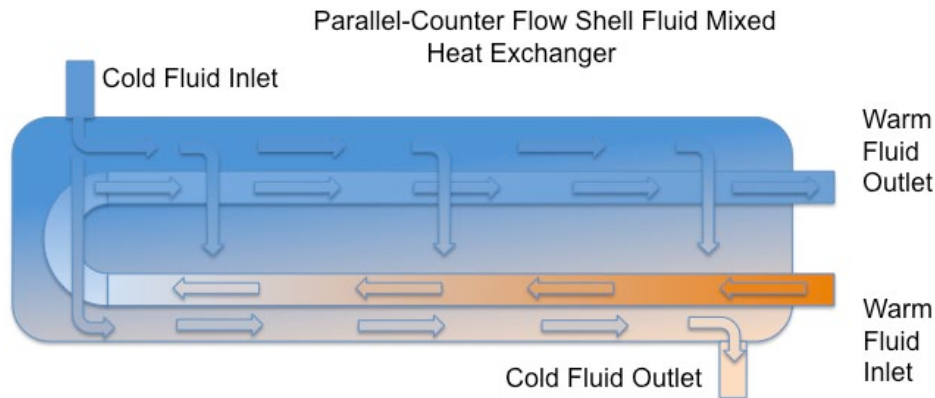


Figure 12.—Illustration of a parallel-counter flow, shell mixed heat exchanger.

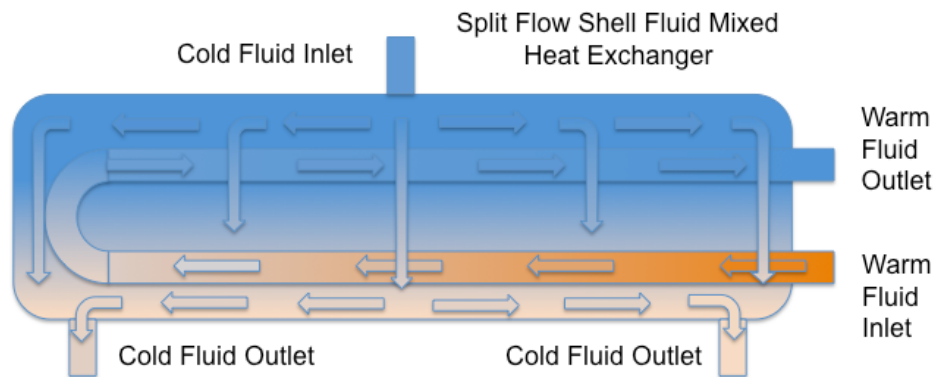


Figure 13.—Illustration of a split flow, shell mixed heat exchanger.

The heat exchanger effectiveness will differ considerably over a range of  $N_{tu}$  for the different heat exchanger geometries, shown in Figures 9 through 13. The heat exchanger effectiveness is given by Equation (11) (Ref. 3) for the ratio of hot to cold fluid capacity rates of 1 as given by Equation (9).

$$\varepsilon = \frac{q}{q_{\max}} = \frac{t_{c,out} - t_{c,in}}{t_{h,in} - t_{c,in}} \quad (11)$$

The heat exchanger effectiveness values, for the different types of heat exchangers are given in Reference 3. The calculated values for a fluid capacity ratio of 1, were plotted and are shown in Figures 14 through 16. Figure 14 shows the effectiveness for counter and parallel flow heat exchangers. This includes two design variations that have characteristics of counter and parallel flow designs. Of the heat exchanger types shown in Figure 14 the counter flow design provides the highest effectiveness values. The effectiveness for the counter flow design exceed the minimum desired effectiveness value of 0.84 at a  $N_{tu}$  of approximately 6 and reach an effectiveness of 0.9 at an  $N_{tu}$  of 9. The other heat exchanger types shown in this figure do not exceed an effectiveness of 0.6 over the range of  $N_{tu}$  shown.

Figure 15 shows the heat exchanger effectiveness for cross-flow heat exchangers. None of the cross-flow heat exchangers, shown in Figure 15, achieve an effectiveness above 0.8, with the cross-flow heat exchanger having both fluids unmixed achieving the highest effectiveness of approximately 0.78.

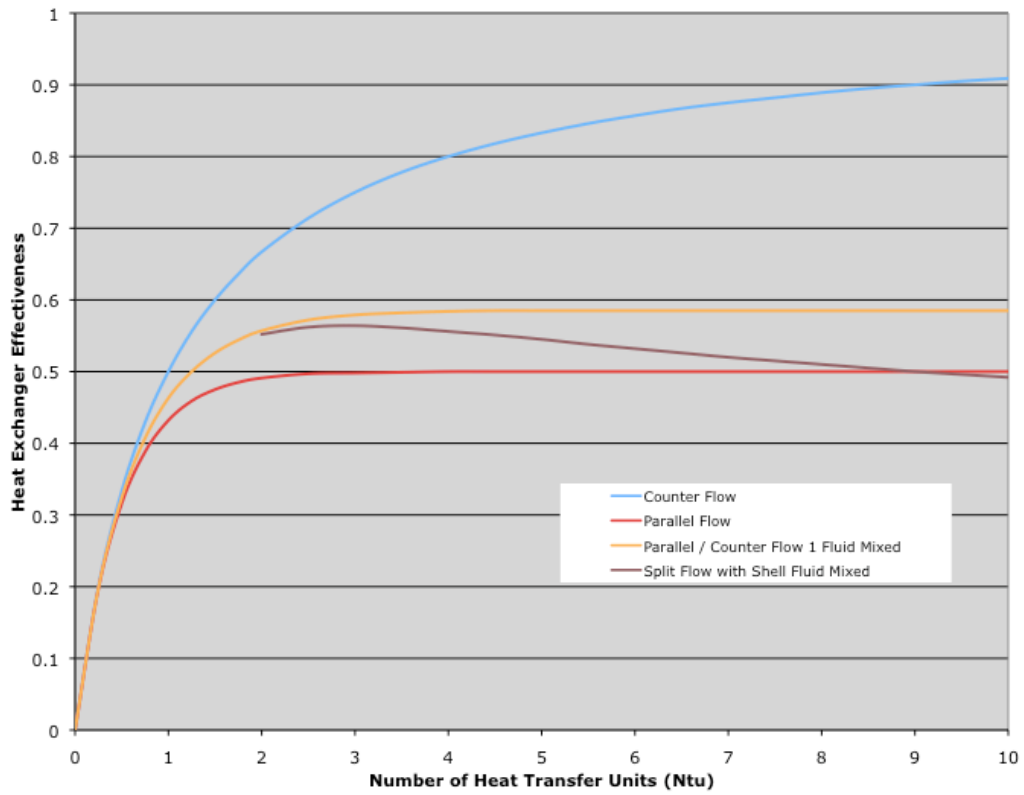


Figure 14.—Heat exchanger effectiveness for counter and parallel type heat exchangers.

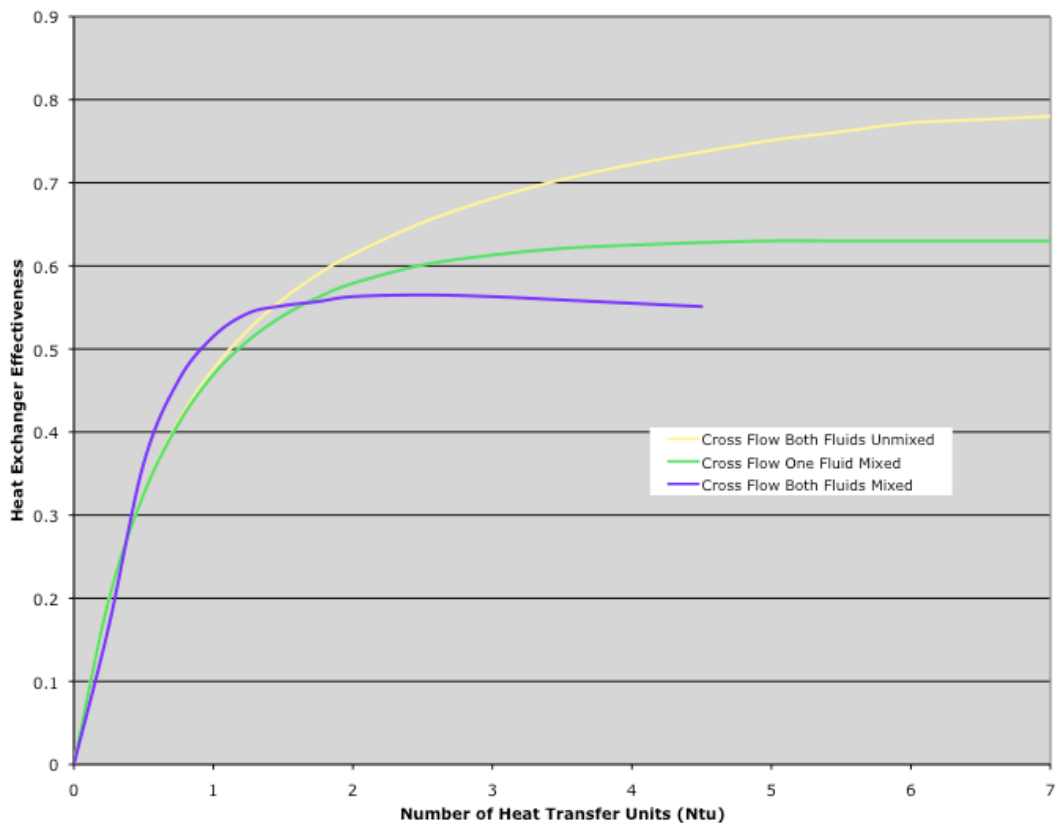


Figure 15.—Heat exchanger effectiveness for cross-flow heat exchangers.

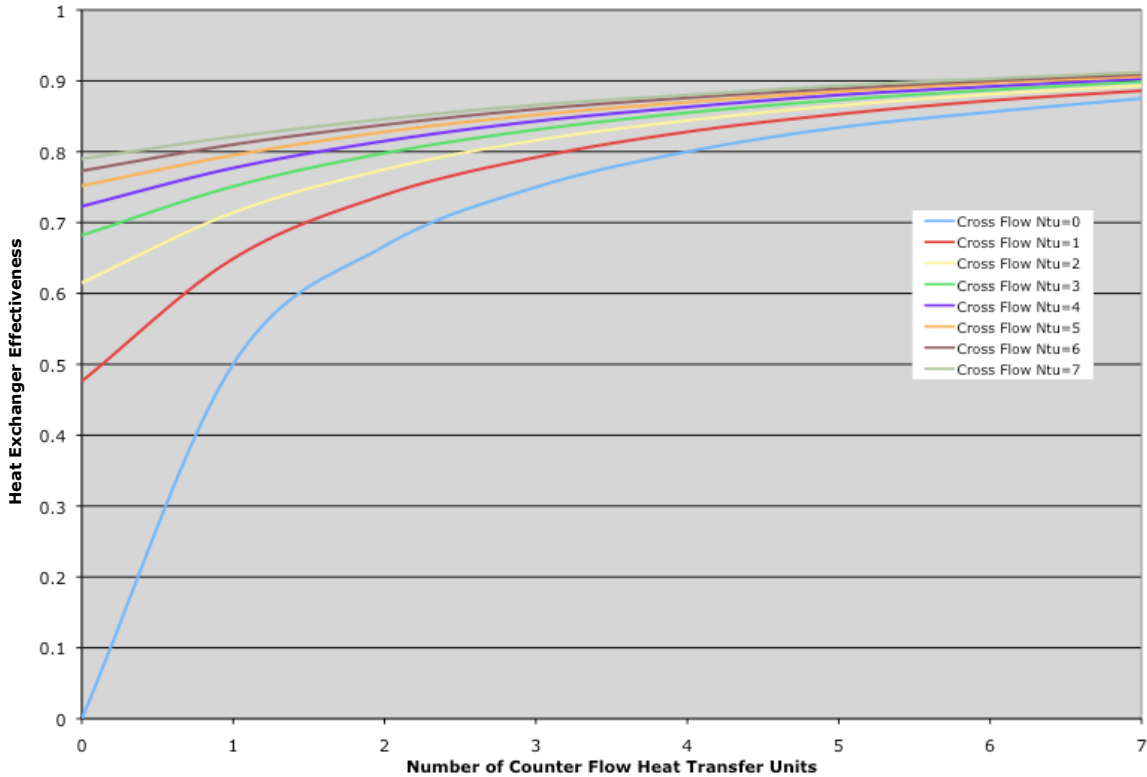


Figure 16.—Heat exchanger effectiveness for multiple-pass cross flow heat exchangers.

Effectiveness values for the last type of heat exchanger are shown in Figure 16. This heat exchanger is a combination of counter-flow and cross-flow type heat exchangers. In this type of heat exchanger, the headers in which the fluid enters and leaves the heat exchanger operate in a cross-flow manner where as the inner core operates in a counter-flow manner. In general, the performance of this type of heat exchanger is better than a cross-flow design but not as effective as a pure counter-flow one.

In practice, it is difficult to construct a true counter flow heat exchanger that has multiple fluid passes. Therefore this combination of cross-flow headers with a counter-flow core better represents the effectiveness of an actual multi-pass counter-flow heat exchanger. From Figure 16, it can be seen that as the cross flow  $N_{tu}$  increases the effectiveness of the heat exchanger increases. The heat exchanger will reach an effectiveness of 0.84 at a counter-flow  $N_{tu}$  of approximately 3 or greater depending on the cross-flow  $N_{tu}$ . The maximum effectiveness is approximately 0.9.

The number of heat transfer units required to achieve the desired effectiveness will determine the overall size of the heat exchanger. This size is based on the total heat exchange area,  $A$ , given by Equation (10). The fluid capacity rate,  $C$ , is given by Equation (12).

$$C = \dot{m} c_p \quad (12)$$

For this design water is used as the cooling fluid. The specific heat of water,  $c_p$ , varies with the temperature of the water (Ref. 4) as shown in Figure 17. However, over the coolant temperature ranges of 20 to 25 °C inlet and 65 °C outlet, the change in specific heat is minimal. Therefore an average specific value of  $c_p = 4,181.3 \text{ J/kg K}$  was utilized in the heat exchanger sizing. The coolant mass flow ( $\dot{m}$  {kg/s}) is given by Equation (2) and is determined based on the desired temperature difference across the fuel cell and its operating power output.

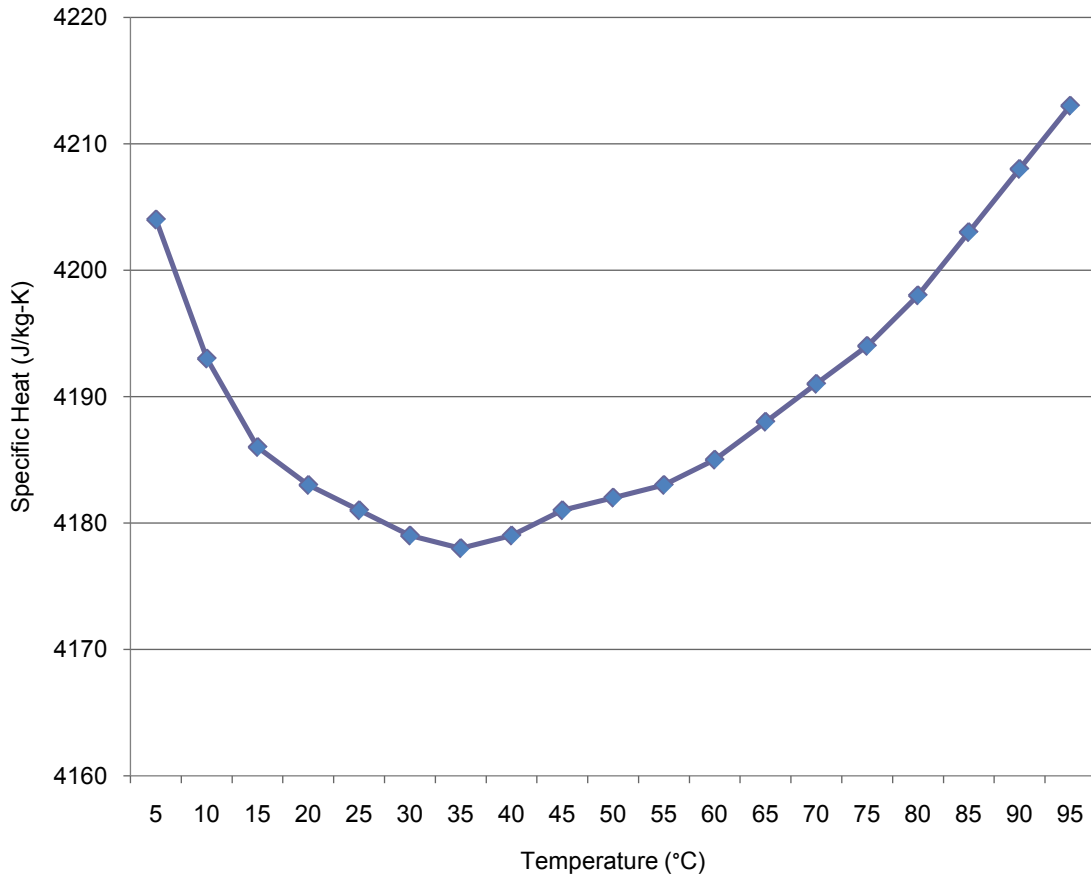


Figure 17.—Specific heat of water as a function of temperature.

The overall thermal conductance of the heat from the warm fluid to the cold fluid ( $U$ , {W/m<sup>2</sup>K}) is given by Equation (13). For this analysis, the heat exchanger wall thickness ( $a$ ) was assumed to be 1 mm and constructed from aluminum with a thermal conductivity of 235 W/mK.

$$U = \frac{1}{\frac{2}{h} + \frac{a}{k_w}} \quad (13)$$

Since the hot and cold fluids are the same, the heat transfer coefficient,  $h$ , is the same for both. The heat transfer coefficient is dependent on the Nusselt number based on diameter ( $Nu$ ) for the flow, given by Equation (14) (Ref. 3). The thermal conductivity of water,  $k_f$ , at 65 °C is 0.656 W/mK.

$$h = \frac{Nu k_f}{d} \quad (14)$$

The value of the Nusselt number will depend on the Reynolds number of the fluid. The Reynolds number ( $Re$ ) is given by Equation (15) (Ref. 3) where  $d$  is the diameter of the fluid passage and  $\mu$  is the viscosity of water at 65 °C, ( $\mu = 4.53 \times 10^{-4}$  N s/m<sup>2</sup>). A fluid passage diameter of 1 cm was used in the subsequent heat exchanger sizing. The same size passage was used for both the hot and cold passages of the heat exchanger.

$$\text{Re} = \frac{4\dot{m}}{\pi d \mu} \quad (15)$$

For Reynolds number values below 2,300 with a constant heat flux, the Nusselt number is a constant value of 4.36. For Reynolds numbers above 2,300 and below  $5 \times 10^6$ , it is given by Equation (16) (Ref. 2). The Prandtl number (Pr) is 2.88 for water at 65 °C.

$$\text{Nu} = \frac{f \text{Pr}(\text{Re} - 1000)}{8 \left( 1 + 12.7(f/8)^{1/2} (\text{Pr}^{2/3} - 1) \right)} \quad (16)$$

The friction factor,  $f$ , is given by Equation (17) (Ref. 2).

$$f = (0.79 \ln(\text{Re}) - 1.64)^{-2} \quad (17)$$

Using the above equations with the specified number of heat transfer units, the heat transfer area, given in Equation (10), can be calculated. This area is then used to determine the required size of the heat exchanger. The heat exchanger length,  $L$ , is given by Equation (18) for a specified number of coolant tubes,  $n_t$ , and the number of passes,  $n_p$ , each tube makes within the heat exchanger. The heat exchanger is arranged so that the cold fluid flows through tubes and the hot fluid flows around the tubes in a counter flow arrangement. The spacing between the tubes is the same as the tube diameter.

$$L = \frac{A}{\pi d n_p n_t} \quad (18)$$

The thickness of the heat exchanger,  $t$ , is given by Equation (19). The thickness is dependent on the number of stacked tubes,  $n_s$ , in the thickness direction.

$$t = d(2n_s + 1) \quad (19)$$

The final heat exchanger dimension, the width,  $w$ , is given by Equation (20).

$$w = d \left( \frac{2n_t n_p}{n_s} + 1 \right) \quad (20)$$

Specifying the tube diameter, number of tubes, passes per tube and how they are stacked will establish the thickness and width of the heat exchanger. The length will vary as a function of the required heat exchange surface area. These values and the subsequent heat exchanger length and width are given in Table 1.

TABLE 1.—HEAT EXCHANGER LAYOUT SPECIFICATIONS

Variable	Value
Tube diameter .....	1 cm
Number of coolant tubes.....	35
Number of passes per tube.....	2
Stacked number of tubes.....	4
Heat exchanger thickness.....	9 cm
Heat exchanger width .....	36 cm

Using the values specified in Table 1 for the heat exchanger, the required heat exchanger length was plotted as a function of the power being dissipated by the fuel cell for various temperature differences across the fuel cell. Graphs were produced for  $N_{tu}$  values of 6 through 10, shown in Figures 18 through 22 respectively.

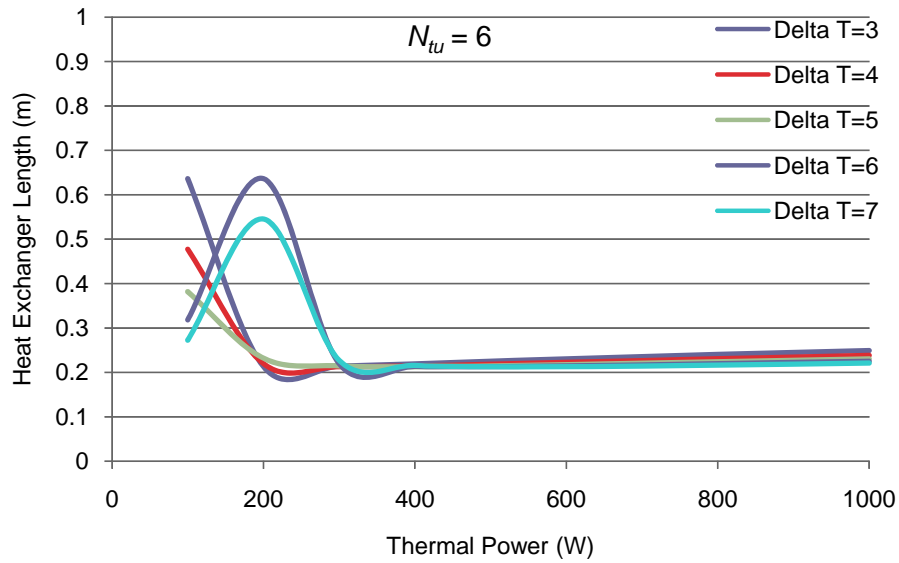


Figure 18.—Required heat exchanger length for  $N_{tu}$  of 6.

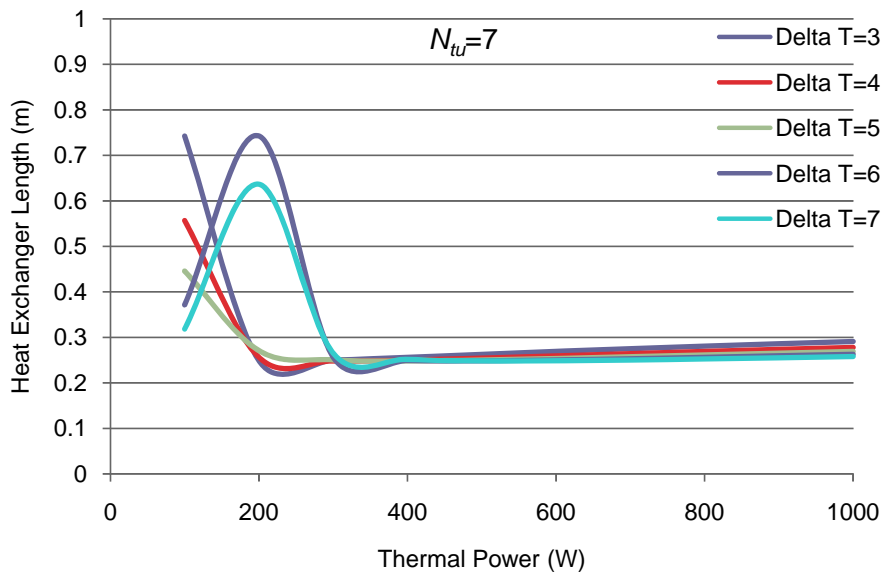


Figure 19.—Required heat exchanger length for  $N_{tu}$  of 7.

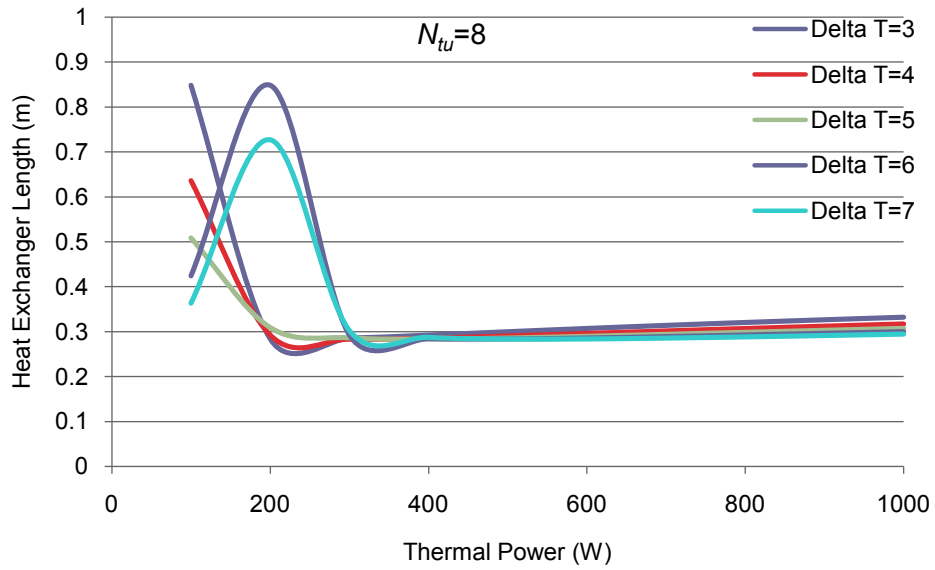


Figure 20.—Required heat exchanger length for  $N_{tu}$  of 8.

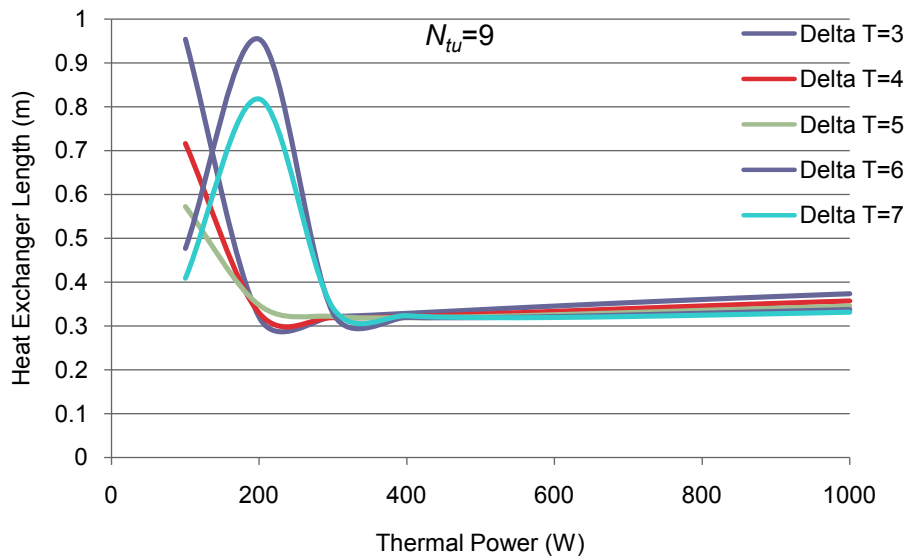


Figure 21.—Required heat exchanger length for  $N_{tu}$  of 9.

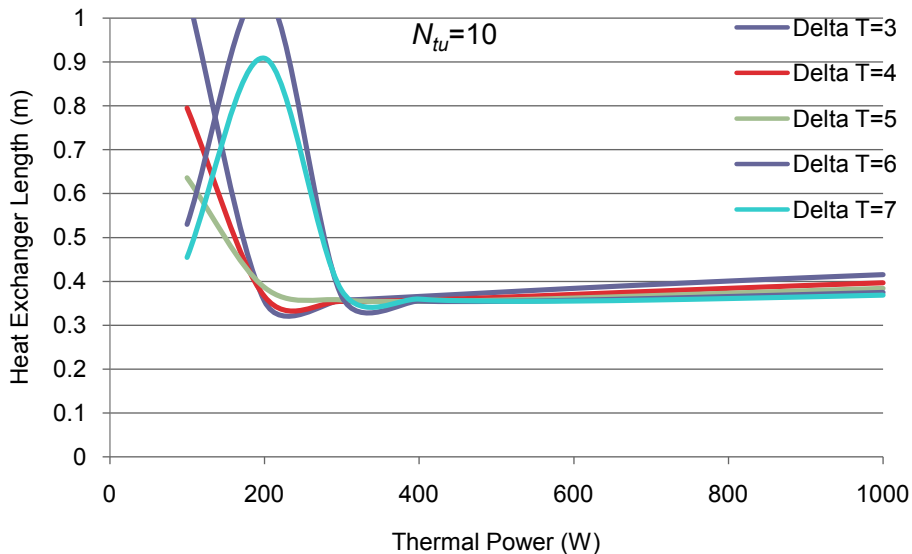


Figure 22.—Required heat exchanger length for  $N_{tu}$  of 10.

The required heat exchanger length results, shown in Figures 18 through 22, follow the same general pattern with increasing thermal power. For a given thermal power level and fuel cell temperature difference (delta T), the required length increases with increasing  $N_{tu}$ , as would be expected. At low thermal power levels, near or below 350 W, the required heat exchanger length increases significantly. This is due to the low mass flow rates required at these power levels, which in turn causes the flow through the heat exchanger to be laminar. To avoid this, a smaller heat exchanger tube diameter could be used to increase the Reynolds number of the flow at the lower power levels. This would induce turbulent flow thereby significantly increasing the heat transfer within the heat exchanger and reducing the required heat exchanger length at the lower thermal power levels.

At thermal power levels beyond 350 W, the required heat exchanger length increases linearly with increasing thermal power. The slope of this increase is low and the slope decreases with increasing temperature difference across the fuel cell. The lower the required temperature difference across the fuel cell, the greater the heat exchanger length. This is expected since the smaller the temperature difference across the fuel cell is achieved by increasing the inlet fluid temperature, which requires a larger heat exchanger area.

## Summary and Conclusion

The analysis has shown that for high heat exchanger effectiveness values, greater than 0.84, the concept of preheating the incoming coolant with the heated exit coolant can achieve and maintain both a fuel cell operating temperature of 65 °C and a minimum temperature difference across the fuel cell. The achievable fuel cell operating temperature was highly dependent on the heat exchanger inlet coolant fluid temperature and allowable temperature difference across the fuel cell. For a heat exchanger effectiveness of 0.9, changes in inlet coolant temperature of 5 °C (from 20 to 25 °C) and a change in the allowable temperature difference across the fuel cell of 2 °C (from 5 to 7 °C) increased the steady state operating temperature of the fuel cell from 65 to 88 °C.

The steady state operating temperature was achieved fairly quickly for the cases analyzed. As would be expected, the lower the effectiveness of the heat exchanger, the lower the steady state temperature and the more quickly it would achieve this temperature. The time to achieve steady state ranged from

approximately 5 sec for a heat exchanger effectiveness of 0.4 to approximately 35 sec for a heat exchanger with an effectiveness of 0.9.

To achieve the high heat exchanger effectiveness values desired, a number of different heat exchanger configurations were considered as shown in Figures 9 through 13. Of these configurations, a counter flow type arrangement was the only configuration that could achieve the required effectiveness range, as shown in Figures 14 and 16. From these figures, it can be seen that the number of heat transfer units for the heat exchanger need to be at least 6 and more likely 9 or 10 depending on the operating requirements. With a  $N_{tu}$  of 9, and the design point values given in Table 1, the dimensions of the heat exchanger would be approximately 0.09- by 0.36- by 0.35-m with a volume of 0.011 m<sup>3</sup>. If a cross flow heat exchanger could be constructed with the desired effectiveness, the required heat exchanger size is reasonable.

This analysis suggests that utilizing a regenerative heat exchanger to maintain the operating temperature and temperature difference within a fuel cell is feasible and worth further study. However, the required high heat exchanger effectiveness indicates that significant heat exchanger design, development, and optimization would be required to produce a system that can meet the desired goals under real world operational conditions.

## References

1. Colozza, A.J. and Burke, K.A., "Fuel Cell Thermal Management Through Conductive Cooling Plates," NASA/TM—2008-215149, May 2008.
2. Incropera, F.P. and DeWitt, D.P., *Fundamentals of Heat and Mass Transfer*, John Wiley & Sons Publisher, 1990.
3. Kays, W.M. and London, A.L., *Compact Heat Exchangers*, McGraw-Hill Publisher, 1984.
4. The Engineering Toolbox, Water-Thermal Properties, [www.EngineeringToolBox.com](http://www.EngineeringToolBox.com), October 2009.

REPORT DOCUMENTATION PAGE			Form Approved OMB No. 0704-0188		
<p>The public reporting burden for this collection of information is estimated to average 1 hour per response, including the time for reviewing instructions, searching existing data sources, gathering and maintaining the data needed, and completing and reviewing the collection of information. Send comments regarding this burden estimate or any other aspect of this collection of information, including suggestions for reducing this burden, to Department of Defense, Washington Headquarters Services, Directorate for Information Operations and Reports (0704-0188), 1215 Jefferson Davis Highway, Suite 1204, Arlington, VA 22202-4302. Respondents should be aware that notwithstanding any other provision of law, no person shall be subject to any penalty for failing to comply with a collection of information if it does not display a currently valid OMB control number.</p> <p>PLEASE DO NOT RETURN YOUR FORM TO THE ABOVE ADDRESS.</p>					
1. REPORT DATE (DD-MM-YYYY) 01-01-2011		2. REPORT TYPE Technical Memorandum		3. DATES COVERED (From - To)	
4. TITLE AND SUBTITLE Evaluation of a Passive Heat Exchanger Based Cooling System for Fuel Cell Applications			5a. CONTRACT NUMBER		
			5b. GRANT NUMBER		
			5c. PROGRAM ELEMENT NUMBER		
6. AUTHOR(S) Colozza, Anthony, J.; Burke, Kenneth, A.			5d. PROJECT NUMBER		
			5e. TASK NUMBER		
			5f. WORK UNIT NUMBER WBS 038957.04.06.02.02.03		
7. PERFORMING ORGANIZATION NAME(S) AND ADDRESS(ES) National Aeronautics and Space Administration John H. Glenn Research Center at Lewis Field Cleveland, Ohio 44135-3191			8. PERFORMING ORGANIZATION REPORT NUMBER E-17567		
9. SPONSORING/MONITORING AGENCY NAME(S) AND ADDRESS(ES) National Aeronautics and Space Administration Washington, DC 20546-0001			10. SPONSORING/MONITOR'S ACRONYM(S) NASA		
			11. SPONSORING/MONITORING REPORT NUMBER NASA/TM-2011-216962		
12. DISTRIBUTION/AVAILABILITY STATEMENT Unclassified-Unlimited Subject Categories: 20, 44, and 15 Available electronically at <a href="http://gltrs.grc.nasa.gov">http://gltrs.grc.nasa.gov</a> This publication is available from the NASA Center for AeroSpace Information, 443-757-5802					
13. SUPPLEMENTARY NOTES					
14. ABSTRACT Fuel cell cooling is conventionally performed with an actively controlled, dedicated coolant loop that exchanges heat with a separate external cooling loop. To simplify this system the concept of directly cooling a fuel cell utilizing a coolant loop with a regenerative heat exchanger to preheat the coolant entering the fuel cell with the coolant exiting the fuel cell was analyzed. The preheating is necessary to minimize the temperature difference across the fuel cell stack. This type of coolant system would minimize the controls needed on the coolant loop and provide a mostly passive means of cooling the fuel cell. The results indicate that an operating temperature of near or greater than 70 °C is achievable with a heat exchanger effectiveness of around 90 percent. Of the heat exchanger types evaluated with the same type of fluid on the hot and cold side, a counter flow type heat exchanger would be required which has the possibility of achieving the required effectiveness. The number of heat transfer units required by the heat exchanger would be around 9 or greater. Although the analysis indicates the concept is feasible, the heat exchanger design would need to be developed and optimized for a specific fuel cell operation in order to achieve the high effectiveness value required.					
15. SUBJECT TERMS Cooling systems; Fuel cells; Heat exchangers					
16. SECURITY CLASSIFICATION OF:			17. LIMITATION OF ABSTRACT	18. NUMBER OF PAGES 24	19a. NAME OF RESPONSIBLE PERSON STI Help Desk (email:help@sti.nasa.gov)
a. REPORT U	b. ABSTRACT U	c. THIS PAGE U			UU



